

An investigation of shear thickening fluids using ejecta analysis techniques

Oren E. Petel^{a,*}, James D. Hogan^b

^a*Carleton University, Department of Mechanical and Aerospace Engineering, Ottawa, ON, K1S 5B6, Canada*

^b*The University of Alberta, Department of Mechanical Engineering, Edmonton, AB T6G 2R3, Canada*

Abstract

In the present study, ejecta dynamics techniques are used to investigate the ballistic response of shear thickening particle suspensions as a means of assessing the particle hardness and the role interparticle friction during penetration. Through particle material variations, the role of particle material strength is discussed primarily through the ratio of the total lateral to total axial kinetic energy of the ejecta field at increasing impact velocities. Two dominant trends are observed in the relation between this ratio of kinetic energy and impact velocity, which are attributed to the properties of the suspended particles. A qualitative model of particle fracture and deformation is proposed to account for the experimental observations. The results of analytical particle strain estimates and computational discrete element modelling of impact ejecta are used to inform the model and discuss the role of interparticle friction in the ejecta field.

Keywords: impact ejecta dynamics, interparticle friction, shear thickening fluids, particle suspensions, ballistic impact, particle image velocimetry, discrete element model

*Corresponding author

Email address: oren.petel@carleton.ca (Oren E. Petel)

1. Introduction

Shear thickening is a common rheological response of dense particle suspensions to shear at elevated strain rates, resulting in a sharp increase in the fluid viscosity. There are several competing theories that attempt to explain the response of these fluids to stimuli and the solid-like behaviour of some suspensions [1, 2, 3, 4, 5, 6, 7]. Recent evidence has shown that reproducing the shear stress response of a discontinuous shear thickening fluid requires consideration of the elastic response within the particle sub-phase of the suspensions, ranging from an elastohydrodynamic coupling of the contact and lubrication forces [8, 9, 10, 11] to an explicit model of frictional contact between particles [6, 12, 13]. In the present study, **we will investigate the relationship between frictional contacts and particle strength within dense suspensions** through an analysis of ballistic impact ejecta. The dynamics of impact ejecta are generally associated with the frictional response of the target material [14], allowing us to isolate these effects on stress transfer through the particle sub-phase of the mixtures during the high-strain-rate loading.

The prevailing theory on the rheological behaviour of dense suspensions is based on the formation of hydroclusters, flow-blocking collections of particles whose dynamics are dominated by hydrodynamic lubrication forces [3, 15]. The hydrodynamic reorganization of particles described by these theories has produced accurate predictions for the onset of shear thickening [16], however, Brown and Jaeger [6, 7] have demonstrated that this hydrocluster-based mechanism is unable to fully explain the discontinuous shear thickening response of dense suspensions. The extension of these hydrocluster models to include the influence of particle stiffness on the suspension behaviour involves coupling the hydrodynamic lubrication forces to the deformation of the particles through the consideration of Hertzian contacts (elastohydrodynamic models) [8, 9, 11]. **These elastohydrodynamic models have been used successfully to model the second shear thinning regime commonly observed following a discontinuous shear thickening transition** [11]. Alternatively, a shear thickening

mechanism involving the dilation of the particle sub-phase [6], which relies on interparticle frictional contacts for stress transfer, provides a consistent framework for observations relating to shear thickening fluids, such as the maximum shear stress and order of magnitude coupling between normal and shear stresses
35 in the fluids [17].

Low velocity impact studies of shear thickening fluids have observed effects that provide direct confirmation of the importance of stress transfer through interparticle contacts. These observations have included a percolating stress front that relates to the motion and spacing between particles, non-hydrostatic
40 stress distributions along container walls [18, 19], and solid-like fracture patterns on the impact surface of the fluid [20]. These relatively low velocity impact experiments, which do not result in notable density changes in the fluid medium, have demonstrated that compressibility of the fluid is not a necessary condition for particle contacts to be formed within an impacted fluid if the volume fraction
45 of particles is sufficient. Using visualization techniques, an effective added mass column of fluid was observed within the impacted suspensions. This added mass column, which extended to form a cone within the suspension, resulted from a network of force chains among particles that spanned the container from the nose of the impactor to the base of the container [18]. This cone of added
50 mass surrounds a central solid plug of material, where the interparticle contacts are more extensive, providing further evidence of the transient development of interparticle contacts. This type of laterally percolating contact front has been visualized in an impacted cornstarch-based shear thickening fluid bed [21].

High-strain-rate characterizations of dense particle suspensions have previously
55 been conducted using a split-Hopkinson pressure bar [22] and plate impact experiments [23]. These studies have observed suspension behaviour that is consistent with the formation of networks of particle contacts within the suspension, resulting from the dynamic loading. In particular, a dynamic shear strength of 500 MPa was measured in a dense suspension of silicon carbide (48% volume
60 fraction) during plate impact testing [23]. These shear stress levels indicate the presence of direct contact force chains among particles [24]. The dynamic onset

of this material strength was related to a compression-induced analog to the dilatancy shear thickening mechanism that consisted of particle networks being formed in a transient process driven by fluid compressibility effects that lead to
65 dynamic jamming of the particle sub-phase [25].

There has been considerable interest in the use of shear thickening fluids for ballistic applications due to the stimuli-responsive nature of the suspensions [26, 27]. Several ballistic studies have noted the influence of particle hardness on the ballistic response of the shear thickening fluids. Kalman et
70 al. [28] found that whether particles were integrated into ballistic fabrics in a wetted (shear thickening) or dry state, the effect of these interstitials on ballistic performance was negligible for the same particle material. However, the ballistic performance of the fabrics was vastly improved when ballistic limit of fabrics integrated with the harder silica particle was compared to the softer
75 polymethylmethacrylate particle. Similarly, the results of ballistic studies on a selection of particle suspensions showed that the increased hardness of the particles resulted in superior resistance to ballistic penetration, deviating significantly from a purely hydrodynamic, inertially-driven response to impact [29, 30]. The combined ballistic results demonstrate that particle interactions within the
80 suspensions appear to dominate the transient behaviour of these fluids.

Although there is clear evidence of the influence of the material properties of the particle sub-phase in the response of dense suspensions, invoking interparticle friction is not absolutely necessary. As a result, differentiating between the elasto-hydrodynamic or frictional models of the interparticle interactions to
85 explain these material responses is challenging. The approach of the present study is to examine the response of these fluids at extremely high **stresses and** strain rates, particularly using impact ejecta analysis techniques, where the ejecta dynamics are known to be **heavily** influenced by interparticle frictional grain contacts [14]. **Under the high stress state impact conditions of the**
90 **present study, the limited elastic strain assumption that is inherent in the elasto-hydrodynamic model formulation is likely no longer valid, as particles undergoing excessive strains cannot maintain Hertzian**

contact, and frictional contact between particles is initiated.

In the present study, we will track the ejecta on the impact face produced
95 by ballistic penetration of shear thickening and dilute suspensions to investigate
the role of interparticle friction during the impact. This technique, which is pri-
marily used in the analysis of impacts relevant to planetary and space science
impacts [31, 32, 33, 34], provides an established approach to determining the
relationships between the target composition and its dynamic behaviour. An
100 impact ejecta analysis may clarify some of the dynamics related to interparti-
cle contacts within these suspensions, particularly under transient high stress
states relevant to ballistic events. The analysis will focus on the influence of
interparticle frictional contacts and particle strength on the relative axial and
lateral distribution of kinetic energy of the ejecta, which will provide a measure
105 of lateral force transfer as a function of the impact velocity. **A discrete ele-
ment computational model of the impact events will be used to help
validate the sensitivity of our chosen kinetic energy ratio parameter
to interparticle friction, particle hardness, and impact velocity for
a dry granular material. A qualitative model of the fluid response
110 will be developed through information gathered from particle strain
estimates, the computational model, and experimental results.**

2. Experimental Configuration

The ballistic impact videos from experiments involving four different particle
suspensions were used in the ejecta investigations in the present study. The
115 experimental configuration involved three components: a gas gun to launch
the projectile, the target capsule, and a high-speed video camera to capture
the trajectory of the ejecta. A smooth-bore single-stage gas gun was used to
launch a 17 grain (1.1 g) chisel-nosed mild steel NATO-standard FSP with an
upper velocity limit of 700 m/s. The target suspension samples were constrained
120 within steel test capsules mounted at the exit of the muzzle. The test capsules
were mounted perpendicular and in close proximity to the muzzle of the gun

(within 5 cm) to reduce projectile yaw. The test capsule had a diameter of 38 mm and a length of 64 mm and the samples were contained within the capsules by a 0.1 mm thick Mylar diaphragms. Although there could be a
125 legitimate concern that the ejecta from the capsules would be influenced heavily by the presence of this diaphragm, the contrasting behaviour observed between the ejecta trajectories for the suspensions cannot be explained simply through the presence of the diaphragm, which was common to all of the experiments. The ejecta resulting from the ballistic penetration of the FSP through the test
130 capsules was tracked using a Photron SA5 high-speed camera at a framing rate of 20,000 fps.

The impact of a projectile on the fluid samples will lead to some lateral divergence of the suspension material as it flows and deforms (see Figure 1), particularly due to the presence of the angled sides of the FSP used in the
135 present study. Naturally, there will be some lateral expansion of the ejecta around the projectile in addition to the axial motion of the ejecta. The ratio of the total lateral kinetic energy to the total axial kinetic energy of the ejecta from the impact face, represented in eq (1) will provide a relative measure of the force transfer within a particle suspension, while the trend of this ratio as a
140 function of impact velocity may provide insight into the mechanics involved in the stress transfer. It should be noted that all impacts above 300 m/s resulted in a complete penetration of the fluid test capsules, which indicates that any yield stresses of the fluids are exceeded by the impacts considered in the present study.

145 *2.1. Mixture Details*

The investigations focused on four different particle suspensions, mixture ratios for which are given in Table 1. These suspensions offer varying volume fractions, ranging from a dilute shear thinning suspension to discontinuously shear thickening suspensions, involving particles with a variation in material
150 properties. The components of the mixtures that were investigated included silica (Fiber Optic Center, monodisperse spheres, $d = 1 \mu\text{m}$), cornstarch (Fleis-

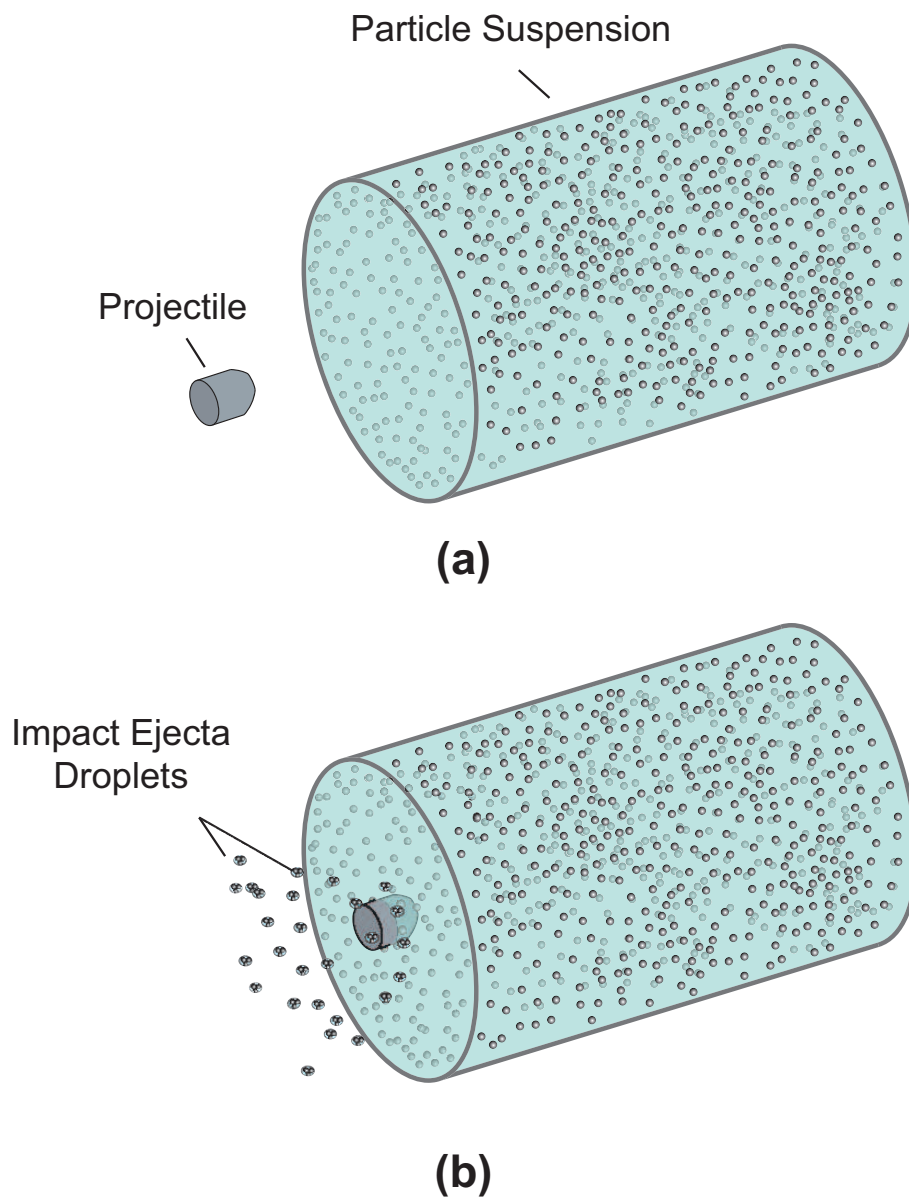


Figure 1: A schematic illustrating the response of the particles in a suspension during a ballistic penetration event (a) prior to penetration and (b) during penetration (cut-away section view).

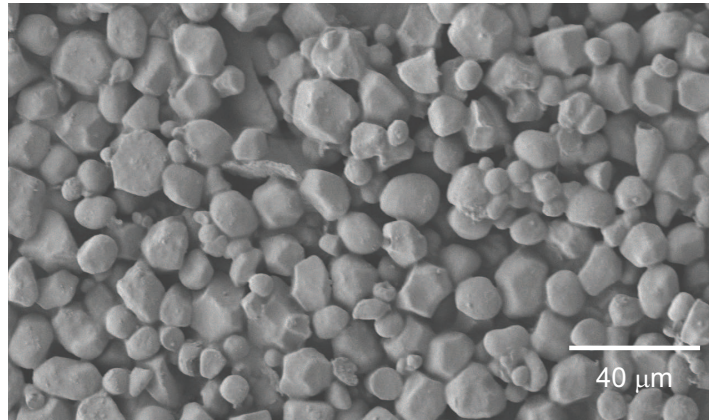
Table 1: The summary of the mixture compositions investigated in the present study.

Sample Name	Solid Component(s)	Solid Mass	Solid Volume	Density
		Fraction (%)	Fraction (%)	(g/cm ³)
Dilute SiC	Silicon Carbide	44.2	21.5	1.57
Cornstarch STF	Cornstarch	62.0	54.0	1.35
Silica STF	Silicon Dioxide	72.5	61.5	1.57
Silica/SiC STF	Silicon Dioxide	50.2	47.6	1.76
	Silicon Carbide	25.5	13.9	

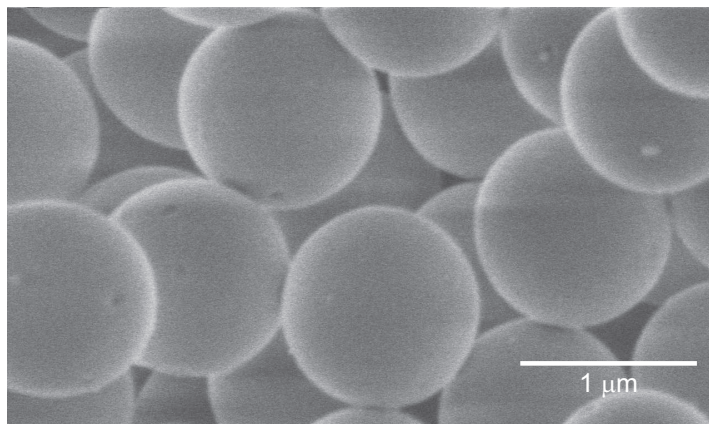
chmann, $d_{\text{mean}} = 10 \mu\text{m}$), and silicon carbide (Washington Mills, irregular morphology, $d_{\text{mean}} = 5 \mu\text{m}$). **Scanning electron microscope images of the particles are shown in Figure 2. Although the silica particles appear to be smooth, based on the sol-gel production method and their void content of 16% [29], the surface roughness of the particles is approximately 0.5% of the diameter. The surface roughnesses of the cornstarch and silicon carbide particles were not estimated.** These particle materials were chosen for their markedly different material properties, particularly their order of magnitude variation in stiffness. The Young’s modulus of cornstarch, silica, silicon carbide are 4.9 GPa [35], 69.3 GPa [36], and 454.7 GPa [36], respectively. Rheological characterizations of the suspensions, as well as that of the ethylene glycol carrier fluid, are shown in Figure 3. Note that three of the mixtures were found to have a discontinuous shear thickening response, while the dilute suspension had a shear thinning response.

2.2. Particle Tracking Methodology

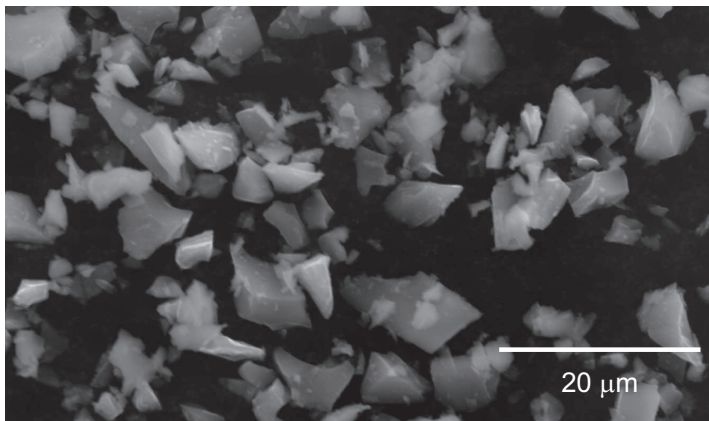
In the present study, our analysis will be limited to the ejecta dynamics of the impact face on the target capsule, as seen in Figure 4. This image shows an impacted capsule where the projectile is moving from left to right as well as the resulting ejecta from the impact. In particle image velocimetry [37, 38], the velocity field is measured by recording the displacement of ejecta of gridded cells across consecutive high-speed video images. In the example image, used in



(a)



(b)



(c)

Figure 2: Scanning electron microscope images of (a) cornstarch, (b) silica, and (c) silicon carbide particles.

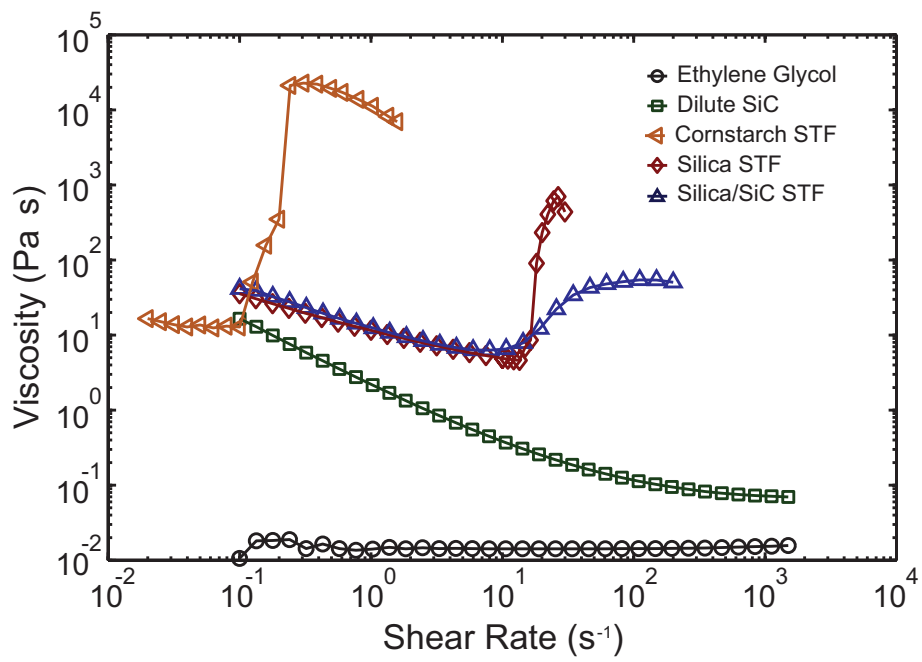


Figure 3: The rheological characterizations of the suspensions in the present study.

the present analysis, the cell-centre locations are shown in blue and the arrows correspond to the measured velocity vectors. The algorithms that are used in
175 this analysis were first developed by Hogan et al. [32, 34] and then later improved for impact fragmentation and ejection of rocks [31].

Ejected droplet sizes are determined using image processing techniques and their centroids are projected onto a velocity field obtained using particle image velocimetry. The ejected droplets (ejecta) are made distinguishable through
180 background subtraction, thresholding, and image enhancements using the image processing toolbox in Matlab [39]. This technique allows us to determine the size, area and centroids of ejecta. The projected area of the droplet on the image is taken as its mass (i.e., no thickness is assumed). Droplet centroids are then projected back onto a velocity field obtained using particle image velocimetry.
185 The corresponding droplet velocity is determined using their weighted distances to the velocity field interrogation points.

The combination of image processing and particle image velocimetry methods allows us to compute the axial and lateral velocities and estimate the mass of the ejecta. In turn, we may then determine the total kinetic energy of ejecta
190 field in each direction. Clearly, the two-dimensional nature of our interrogation will result in an underestimate of the true lateral velocity field since we are unable to determine the resultant radial velocity component due to out-of-plane ejecta motion. For consistency, the same limitation was placed on our analysis of the computational model that will be presented in a subsequent section.

195 **3. Experimental Results**

The results of the ejecta analysis can be represented in several forms, one common form of which is using a cumulative distribution function representation of the resultant eject velocity, a sample of which is shown for the impact face of the cornstarch mixture in Figure 5. The cumulative velocity curves look quite
200 similar among the various mixtures and an in-depth analysis of those curves will not provide additional insights into the response of these suspensions, in

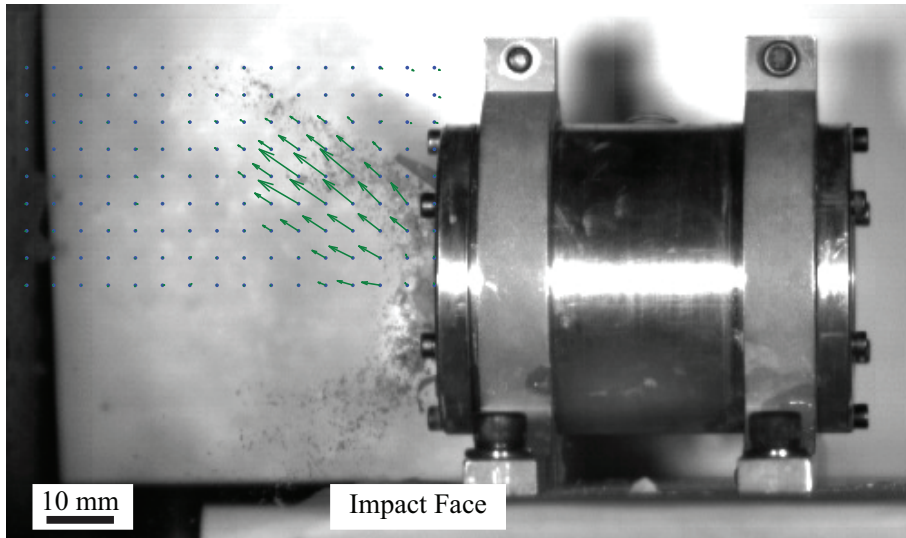


Figure 4: High speed photograph of the impact ejecta with gridded particle image velocimetry interrogation locations (blue dots) and the corresponding velocity vector field (green arrows) at the impact face.

particular, the role of interparticle friction beyond previous discussions relating particle hardness to performance.

Rather than looking at the resultant velocity distribution within the ejecta
 205 field, we will focus our attention on the ratio of the total lateral to total axial
 kinetic energy in the ejecta field. Investigations of ejecta dynamics have demon-
 strated that the angle of the ejecta relative to the free surface is directly related
 to the friction within the flow of the ejecta [14, 40]. This kinetic energy ratio is
 a parameter that provides another measure of the lateral force transfer, which
 210 may differ considerably in the presence of friction and is proposed as an alterna-
 tive to flow angle for ejecta resulting from impacts of non-spherical projectiles.
 We can define this global kinetic energy parameter by the expression

$$\alpha = \frac{\sum KE_{yi}}{\sum KE_{xi}}$$

$$KE_{yi} = \frac{1}{2} m_i V_{yi}^2 \quad (1)$$

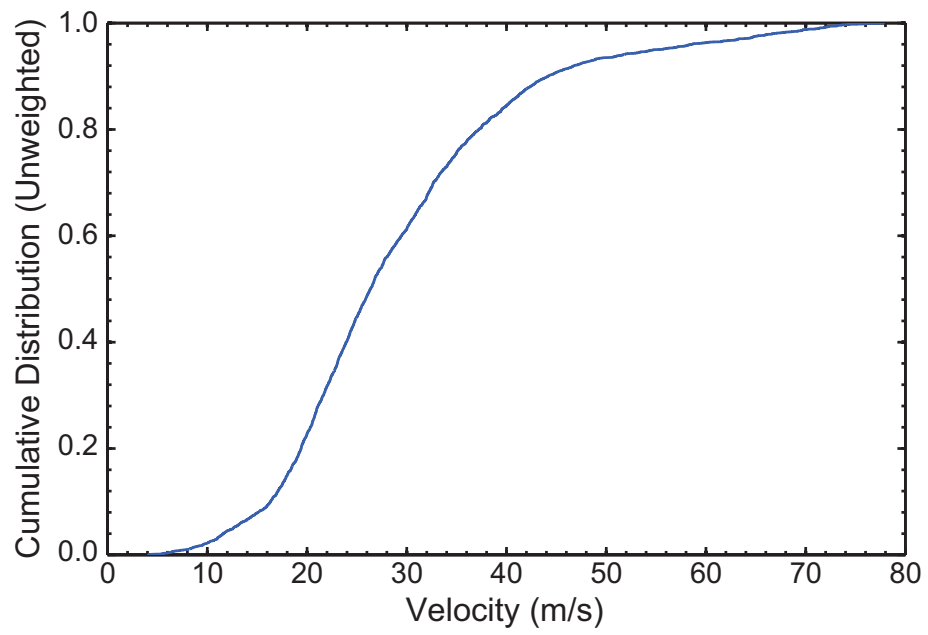


Figure 5: A plot of the cumulative distribution function for the impact face ejecta velocity from a 405 m/s incident projectile velocity into the Cornstarch STF.

$$KE_{xi} = \frac{1}{2}m_iV_{xi}^2$$

where KE_{yi} , KE_{xi} , m_i , V_{yi} and V_{xi} are the lateral kinetic energy, axial kinetic energy, mass, lateral velocity, and axial velocity of the i^{th} ejecta droplet, respectively. The cumulative distribution of the lateral to axial kinetic energy of individual droplets is shown in Figure 6. Note that this kinetic energy ratio biases to lower lateral dispersion of the droplets for the softer particle materials at a given velocity, which may have been expected based on elasto-hydrodynamic considerations without invoking arguments pertaining to direct interparticle contacts or friction. A global representation of this ratio through the α parameter, as defined by equation (1), provides an alternative approach to analysing the kinetic energy distribution in the ejecta field. The value of α for the impact-face ejecta field for each mixture is shown at varying incident FSP impact velocities in Figure 7. The error bars in this figure represent the measurement error pertaining to the data collection and not the statistical scatter in the ejecta plume. There is some error related to determining these ratios since material motions in the plane of the camera line of sight cannot be resolved. Therefore, the analysis is restricted to ejecta with minimal motion along a vector into or out of the images, which would add to the lateral kinetic energy of the ejecta. As a result, we are restricted to analysing a relatively small segment of the total ejecta. Therefore, absolute parameter values are less important, while general and relative trends in the data are seen as meaningful.

A comparison of the α parameter for the mixtures investigated is consistent with the cumulative distribution representation of the individual droplet kinetic energies, following a general stiffness-based classification of the data. There are two trends that are evident in the α parameter as a function of the incident FSP velocity that may provide insight in the suspensions response at high strain rates. The dilute suspension of silicon carbide and cornstarch STF both show no evident variation in the α parameter at increasing impact velocities, meaning that the global ratio of lateral to axial kinetic energy of the ejecta is unchanged. Although, the relative values of the α parameter shows that the higher volume

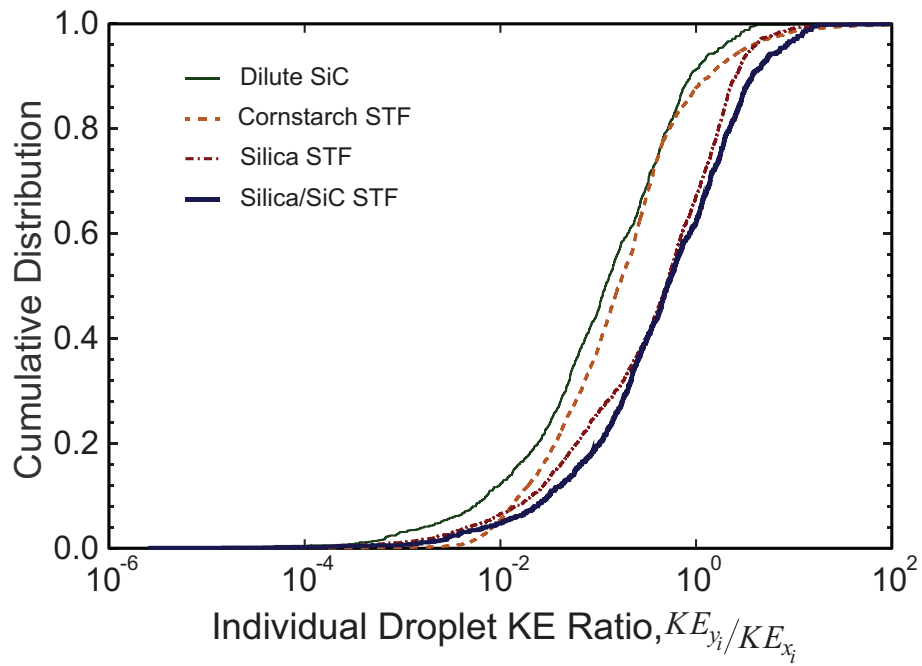


Figure 6: A plot of the cumulative distribution function for the lateral to axial kinetic energy ratio of the individual droplets within the impact face ejecta from a 405 m/s incident projectile velocity into the various test mixtures.

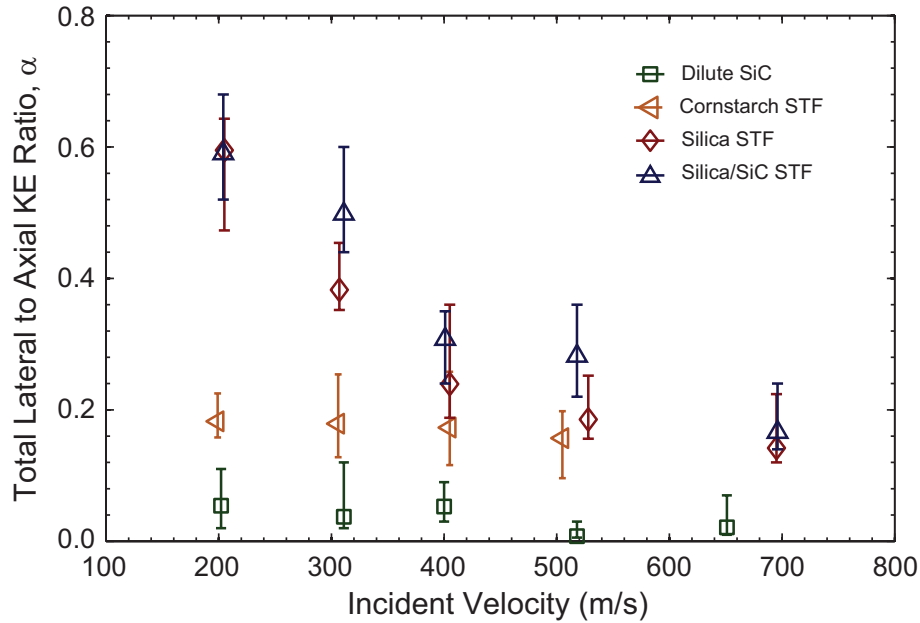


Figure 7: Comparison of the ratio of lateral to axial kinetic energy of ejecta on the impact face of the sample as a function of the impacting velocity for the particle suspensions tested.

fraction in the cornstarch STF leads to more significant lateral kinetic energy in the ejecta plume. In contrast, the silica and silica/silicon carbide STFs exhibit much larger values of the α parameter at lower velocities, which was to be expected based on particle strengths **and hardness**, however they also display a rapid decay in the global lateral kinetic energy within their ejecta field. **These results would suggest that particle hardness becomes important for lower impact velocities.** The ejecta field from the impact face is directly related to the stress distribution within the impacted fluid at this surface, which is causing the expansion of this ejecta plume. The two distinct trends seen in the experimental data may provide insights into the stress transfer within these fluids at high strain rates.

The penetration experiments resulted in some noteworthy qualitative observations of the material behaviour as well. Previous impacts on shear thickening fluids at low velocities demonstrated the propagation of surface cracks that ap-

peared to show a mode-1 fracture patterns on the impacted surface [20]. In the present study, the impact surface was not imaged at the appropriate angle to discuss similar surface features on impact; however, it is worth noting that immediately following a penetration experiment with the three STF mixtures, we observed a short-lived hole in the fluids reminiscent of a shear-dominated plugging failure mechanism (mode-2 fracture). Although the hole initially appeared stable, within tens of seconds, the material surrounding the penetration path would eventually appear to “melt” back to its initial state. We interpret this as evidence that the carrier fluid (ethylene glycol) returned to the material surrounding the hole, fluidizing the particle bed.

3.1. Estimates of Particle Strain During Impact

To obtain reasonable estimates of the strain among the particles, a simple one dimensional impedance matching calculation can be used to determine the maximum stress within the fluids following an impact. This is a simplification of the response of the interaction between the projectile and fluids, although without proper shock Hugoniot data for each mixture, this approach provides an order of magnitude accurate estimate of the maximum stress within the fluids immediately following the impact. Based on shock Hugoniot data obtained for similar mixtures[23], as well as Hugoniot mixture theories [41], the sound speeds of the mixtures tend toward the bulk sound speed of the liquid component of the mixtures, ethylene glycol (1850 m/s [23]). Using this approximation rather than the true shock Hugoniot of the mixtures results in an underestimate of the maximum stress state due to the impact. Using an impedance matching approach, the stress at the impact face is approximated by the expression,

$$\sigma = \frac{Z_1 Z_2}{Z_1 + Z_2} \cdot u_i \quad (2)$$

where σ is the estimated impact stress at the nose of the projectile, Z is the acoustic impedance, u_i is the impact velocity, and the subscripts

Table 2: Estimates of particle strains resulting from a projectile impact at 200 m/s.

Sample Name	Z (kg/m ² s)	Max. Stress (MPa)	Particle Strain (%)
Dilute SiC	2.9x10 ⁶	540	0.1
Cornstarch STF	2.5x10 ⁶	470	9.5
Silica STF	2.9x10 ⁶	540	0.8
Silica/SiC STF	3.3x10 ⁶	600	ϵ_{SiO_2} - 0.9 ϵ_{SiC} - 0.1

Table 3: Estimates of particle strains resulting from a projectile impact at 700 m/s.

Sample Name	Z (kg/m ² s)	Max. Stress (MPa)	Particle Strain (%)
Dilute SiC	2.9x10 ⁶	1880	0.4
Cornstarch STF	2.5x10 ⁶	1630	33.4
Silica STF	2.9x10 ⁶	1880	2.7
Silica/SiC STF	3.3x10 ⁶	2100	ϵ_{SiO_2} - 3 ϵ_{SiC} - 0.5

1 and 2 represent the projectile and fluid, respectively. The acoustic
 285 impedance is defined as the product of the density and sound speed
 of the material. Using an impedance value of 35.5x10⁶ kg/m²s for
 the steel projectile based on bulk sound speed, we can estimate the
 maximum stresses within the various suspensions at the moment of
 impact. Using these values for the impact stress, an estimate of
 290 resulting particle strains can be made based on the elastic properties
 of the particles and the expectation that particles participate in stress
 transfer through the fluid. These results of these estimates are shown
 in Table 2 and Table 3 for impact velocities of 200 m/s and 700 m/s,
 respectively.

295 These order of magnitude estimates provide insight into the be-
 haviour of the particles within the fluids during impact. For instance,
 an examination of the strain estimates among the cornstarch parti-
 cles demonstrates that particle strain varies between 9-33%. The

integrity of a cornstarch particle is lost as a result of the impact. At
300 these compressive strains, for both impact limits, the response of the
cornstarch is no longer elastic. Similarly, the estimate of strain for
the silica particles suggests that they may also be in the range where
fracture or plastic deformation of the particles are possible, particu-
larly at the higher impact velocities. Moreover, these estimates show
305 that the assumption of elastic deformation involved in the Hertzian
contact formulation of elasto-hydrodynamic theory is violated in this
dynamic range for cornstarch and possibly for silica. Hertzian con-
tact mechanics are only valid in the range of small elastic deformation
of interacting materials. Excessive particle deformation necessitates
310 considering frictional contacts between particles. It should be noted
that these strain estimates and the conclusions drawn from them with
regards to the validity of Hertzian contact within an STF is confined
to the present study or fluids in a similar dynamic stress state and
not generalized for rheological flows.

315 4. Computational Model

A simplified computational model of the experiments was investigated to
provide insight into the relationship between the total kinetic energy ratio and
the material properties of a packed granular bed, in particular the relative roles
of particle stiffness and roughness. Impact ejecta studies have shown that an
320 increased frictional response within ejecta leads to a broader ejecta plume [14,
40]. Investigations involving impact ejecta flow typically consider the flow angles
of the target material following an impact with a spherical impactor. In the
present study, we had used a cylindrical FSP, meaning that the ejecta flow
angles from the impact may vary due to the orientation of the cylinder, not
325 discounting the possibility of yaw angle influences. As a result, our investigation
focused on a global lateral dispersion metric that consists of a ratio of the
total lateral kinetic energy to the total axial kinetic energy in the ejecta field

(equation 1). **We will use this computational model to provide insight into the relationship between interparticle friction, particle stiffness, and impact velocity and the ratio of kinetic energies obtained from our experimental investigation.**

The computational domain and approach is similar to a previous study on impact cratering in granular materials [42]. A commercial multiphysics software package, LS-DYNA, was used to model the impact [43]. A screenshot showing the initial orientation and impacted target at the impact face are shown in Figure 8. The computational domain consisted of the impactor that was modelled as a rigid steel cylinder, the target material that consisted of approximately 90,000 discrete elements, and a lateral rigid confinement of the target material. There was no axial confinement of the target material on the backface. The target material was modelled using a discrete element approach that enabled explicit control of the interparticle friction within the packed discrete element granular bed. If we consider the relative size of the particles in the discrete model of the target to the impactor, the diameter range of the discrete particles would be equivalent to 300-400 μm . The frictional contact between particles was controlled using the *CONTROL_DISCRETE_ELEMENT card, which allowed for direct control of this parameter [43]. The friction coefficients for the calculations were set to either 0 or 0.8, which corresponds to smooth (frictionless) and rough particles respectively. The individual particles were modelled using the *MAT_ELASTIC card with a density of 2200 kg/m^3 and a Young's modulus of 70 GPa and 7 GPa for the hard and soft particles, respectively. The identical distribution of discrete elements was used in every simulation to ensure that differences in the microstructure of the particle bed did not influence the results. Three particle types were investigated: (*i*) hard particles with surface roughness; (*ii*) hard particles with smooth surfaces; and (*iii*) soft particles with rough surfaces. **The interstitial fluid of the suspensions was neglected in these simulations as the purpose was not to build a model with absolute physical fidelity able to reproduce the complete spectrum of fluid behaviour, including the rheological response of these fluids,**

**but rather to validate the use of the α parameter and its sensitivity
360 to particle roughness, stiffness, and impact conditions.**

For smooth particles, the forces between the particles are Hertzian, consistent with the elastohydrodynamic framework discussed in the context of dense shear thickening suspensions. The forces between particles act through their center of mass. In the case of frictional particle contacts, the forces between
365 particles may have a rotational component since the force vectors do not necessarily run through the center of mass for the particles. The impactor velocity was varied between 300-700 m/s and an ejecta sample size of 1400 particles was used for the analysis. The cumulative distribution of the kinetic energy ratio for the discrete elements is shown in Figure 9 for the three particle types investigated. The α parameter variation within the ejecta field as a function of the
370 impactor velocity is shown for the three particle types in Figure 10.

The results show the discrepancy in the ratio of the total lateral kinetic energy to total axial kinetic energy of the ejecta field for the smooth and rough particles at different impactor velocities. Given the simplifications inherent in
375 the model, the actual values calculated from the simulations should not be compared directly to experimental results reported previously. The purpose of these calculations was to investigate the general sensitivity of this kinetic energy parameter to the presence of interparticle friction and particle hardness within the ejecta field. Although there is some variation in the kinetic energy parameter,
380 the calculations show that the presence of interparticle friction results in a considerable increase in this ratio, which is indicative of increased lateral force transfer within the particle bed. The result relating friction to increasing lateral force transfer is consistent with the previous impact ejecta studies[14]. The influence of the rigidity of the particles on the kinetic energy parameter was also
385 investigated using this simplified computational model. For comparison, the Young's modulus of the rough particles was varied between 7 GPa and 70 GPa for the soft and hard particles, respectively. The results from the simulations show that the roughness of the particles has a stronger influence on the ejecta dynamics than the particle rigidity. **Additionally, the computational re-**

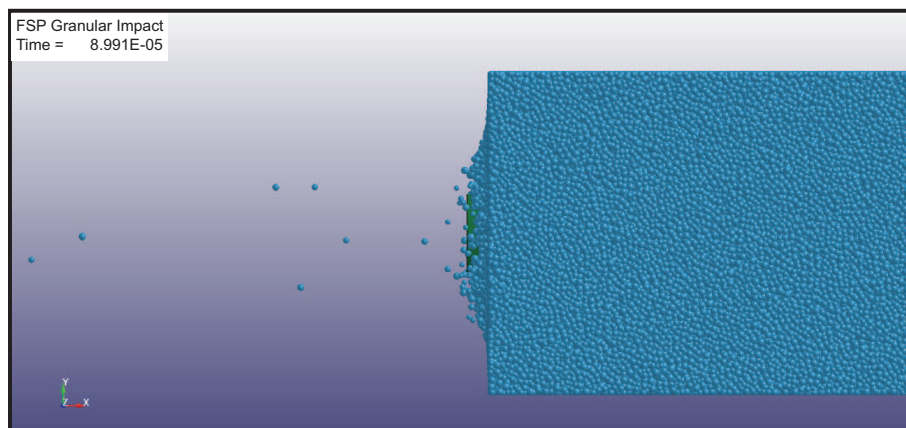
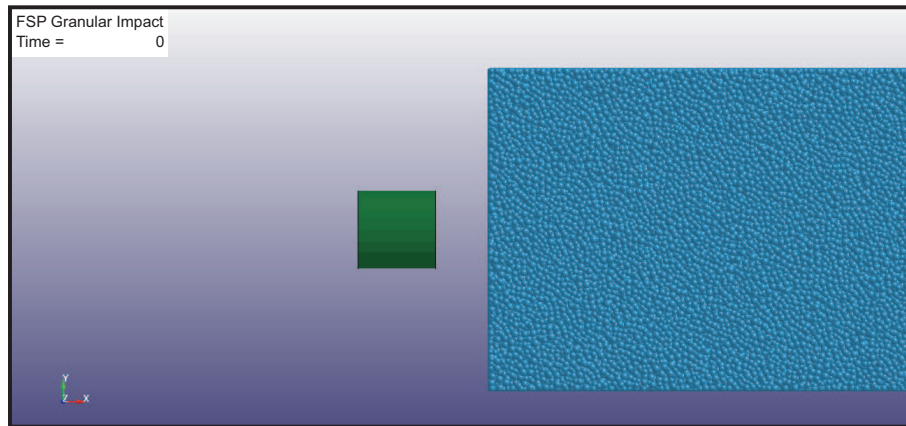


Figure 8: A screenshot of the impact face of the LS-DYNA model of the impact ejecta investigation of the present study.

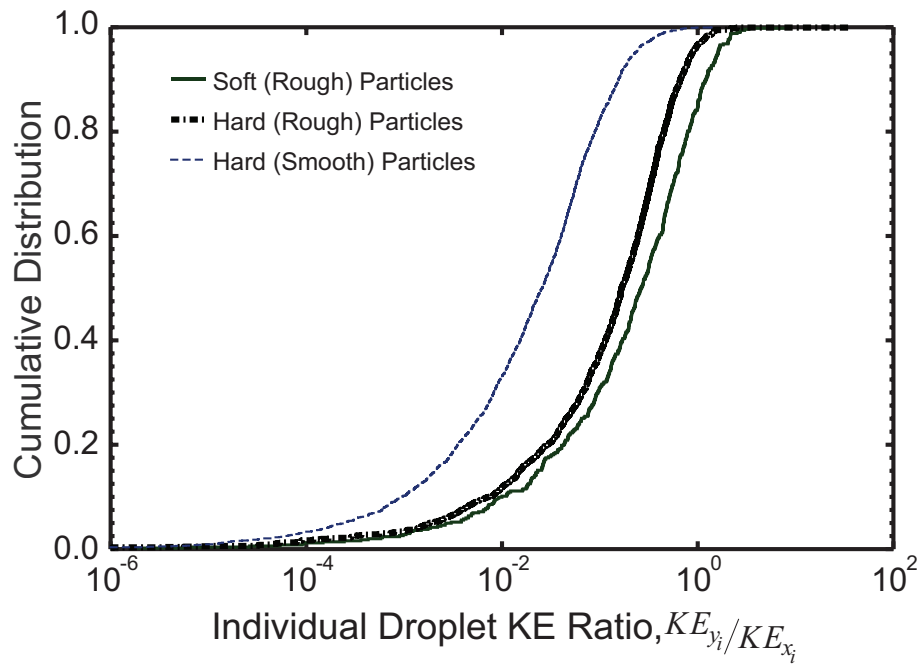


Figure 9: A plot of the cumulative distribution function for the lateral to axial kinetic energy ratio of the discrete elements within the impact face ejecta from a 400 m/s incident projectile velocity calculated for the various particle types using LS-DYNA.

390 **sults further suggest that softer particles will result in a higher ratio**
of kinetic energies. It should be noted that the α parameter is relatively con-
stant with impactor velocity for all three particle types, although there is some
variation around a mean value without a clear trend. These computational
results will provide useful guidance in the interpretation of the experimental
395 ejecta measurements shown previously.

It should be noted that these calculations have some important
limitations that need to be recognized when comparing the results
from the model to experiment. The main limitation is the use of
single element elastic particles, which are unable to deform and cap-
400 **ture effects of fracture or plasticity among particles. As the esti-**
mate of particle strains has shown in the preceeding section of this
manuscript, particle strains are expected to be significant among the
impacted particles, particularly at higher impact velocities. While
our future efforts will focus on refining this model, for the purpose of
405 **the paper, the model suffices to qualify the link between the α kinetic**
energy parameter and the presence of friction and particle stiffness.

5. Discussion

Ejecta velocity angles, which are commonly measured in hypervelocity ejecta
plumes [14], are typically defined from the free surface of the material being im-
410 pacted, where the trend of increasing friction within the ejecta results in a de-
creasing ejecta angle (i.e., a laterally broader plume) [40]. In the present study,
we use the ratio of total lateral to total axial kinetic energy, which would be
directly related to the angle complimentary to the traditional ejecta angle defi-
nition from hypervelocity impact investigation. Therefore, the effect of greater
415 internal friction within our samples should result in an increase in this kinetic
energy ratio. Our simulations of a model packed-bed granular system confirms
that the presence of intergranular friction is in fact related to the global distribu-
tion of lateral kinetic energy in the ejecta field represented by the α parameter.

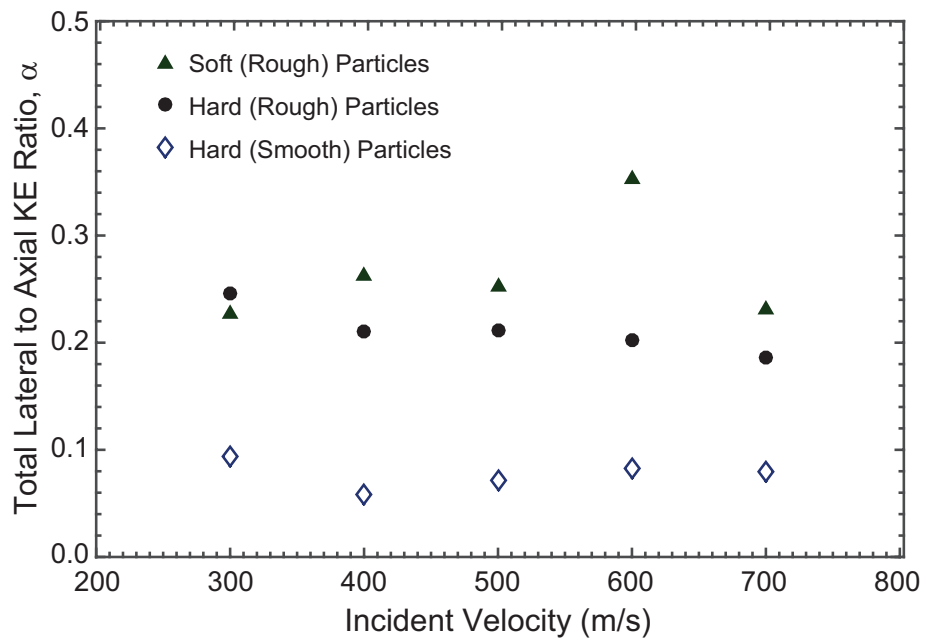


Figure 10: The total kinetic energy ratio as a function of the incident impact velocity of the FSP on a packed bed of smooth ($\mu = 0$) and rough particles ($\mu = 0.8$). Soft and hard particles had elastic moduli of 7 GPa and 70 GPa, respectively.

The experimental ejecta analysis involved four particle suspensions, three
420 of which exhibit shear thickening rheological behaviour based on Figure 3. If
we analyse the impact face ejecta (Figure 7), we see two distinct trends among
the data. The first noticeable trend is that for two of the suspensions, the
dilute SiC and Cornstarch STF, the ratio of total lateral to axial kinetic energy
is either constant or slightly decreasing with increasing impact velocity of the
425 projectile. Therefore, increasing the impact velocity results in negligible changes
to the lateral force transfer in the suspensions at the impact face. Recall that
the impact face ejecta is moving in the opposite direction with respect to the
projectile motion, meaning that the ejecta is driven exclusively by the stress
state within the impacted fluid. This relationship between the ejecta and the
430 stress state makes the impact face an insightful focus for our discussion of the
role of interparticle friction within these suspensions at high strain rate.

The dilute SiC suspension should respond hydrodynamically to the im-
pact [29, 30], as extensive interparticle contacts are not expected, and the rel-
ative lateral to axial force transfer in the fluid should be independent of the
435 impact strength. If we contrast the dilute suspension ejecta with the results
from the impact with the cornstarch STF suspension, we notice that the corn-
starch suspension responds to the impact with a greater proportion of lateral
kinetic energy. The increased lateral force transfer and resulting ejecta in the
shear thickening fluid as opposed to the dilute suspension is consistent with the
440 observations of low velocity impact experiments on similar suspensions [18, 19].
As the impact velocity increases, the stresses transferred within the suspension
increase as well, including the lateral stresses. If these principal stresses vary
proportionally, then it would be expected that the ratio of lateral to axial kinetic
energy of the ejecta would not vary significantly with impact velocity, which is
445 seen in the computational results.

The second trend that is apparent in the ejecta data shows a significant rel-
ative decrease in the lateral kinetic energy of the ejecta with increasing impact
velocities. This trend is seen in the ejecta data from suspensions containing el-
evated volume fractions (61%) of silica or a mixture of silica and silicon carbide

450 particles that exhibit shear thickening rheological behaviour (Figure 3). At the
lowest impact velocities tested, the ejecta data shows evidence of considerable
lateral force transfer within these two suspensions. The relative ratio of kinetic
energy in the lateral direction of these silica-based suspensions is approximately
3 times larger than ratio of lateral kinetic energy in the cornstarch-based sus-
455 pension. This would indicate that the lateral force transfer is more efficient
with these two silica-based suspensions in comparison to the cornstarch-based
suspension. **One may conclude that these results can be adequately
explained through the disparity in the stiffness of the silica, silicon
carbide, and cornstarch particles, however, the computational results**
460 **show a different trend (Figure 10). The computational model yields a
slightly higher value of α , the kinetic energy ratio, for soft particles.**
**Therefore the computational model indicates that particle stiffness
alone does not explain the experimental results.** Comparing the value
of α for the various suspensions (Figure 7) to the results obtained with the
465 computational model (Figure 10), it would seem that interparticle friction has
a significant role regarding stress transfer within the silica and silica/silicon
carbide STFs under these impact conditions.

**The morphology of the cornstarch particle (cuboid) would indi-
cate that friction would not be negligible within the cornstarch sus-
470 pensions. However, the relatively low material strength of the corn-
starch, resulting in plastic yield behaviour, may limit the influence of
friction and material stiffness on the ejecta fields for these mixtures.**
**The computational results suggest that the soft particles, such as the
cornstarch particle, should have had the highest α parameter based**
475 **on particle stiffness (Figure 10). Strain estimates show that any corn-
starch particles participating in stress transfer would be deforming
plastically at these estimated strain levels.**

One could argue that the volume fraction of the silica-based suspensions
may dominate the efficiency of the lateral force transfer, however comparing the
480 trends of the two silica-based suspensions, which both have identical particle

volume fractions, show that significant variations in lateral force transfer exist among suspensions with identical volume fractions. These variations are considerably larger than the variation of the α parameter seen within the results for the cornstarch suspension itself. Similarly, the role of suspension inertia cannot
485 be used to explain the relative responses of the various suspensions. Consider that the Silica STF suspension has the same mixture density as the Dilute SiC suspension, yet their behaviour could not be more different. Furthermore, if we consider the response of the ejecta from the two silica-based suspensions at the lowest impact velocity, there is also no discernible difference in their responses
490 despite the fact that the mixtures have different densities (see Table 1). However, under increasing impact velocities, these two suspensions show significant variations in their ejecta response. This decreasing kinetic energy ratio with increasing impact velocity is not predicted by the computational model for any of the particle types, regardless of particle surface roughness or stiffness.

495 A decrease in the relative lateral kinetic energy at increasing impact velocities signifies a reduction in the lateral stress transfer through the suspension, implying that there is a breakdown within the mechanism of stress transfer. If the lateral stress transfer in the fluid was completely dominated by hydrocluster formation and lubrication forces, the lateral stress transfer through the suspension should not be strongly affected by increased stress loading in the
500 silica or silica/silicon carbide STFs. **Elastohydrodynamic theory does predict a shear-thinning response within STFs beyond the critical shear rate [10, 11], which depends on the elastic modulus of the particle materials. While it is possible that elastohydrodynamic theory may be**
505 **able to explain the behaviour of the ejecta through particle stiffness arguments and the transition to shear thinning responses, our earlier strain estimates indicate that the elastic assumption inherent in the model is not valid for cornstarch. On a conceptual basis, the idea of particle strength-dominated destruction of particle contact networks**
510 **is consistent with this theory and our experimental results.**

At increasing strains, the contact area between the particles neces-

sitates invoking friction in the discussion, as particles can no longer be thought of as frictionless. If we consider that the lateral stress transfer through the suspension is partially explained by interparticle frictional contacts, then increasing the impact velocity of the projectile could lead to deformation of the particles, as the stresses transferred through the contact points could vary by orders of magnitude. Significant deformation of the particles, either elastic or plastic, would result in a reduction of the lateral force transfer within the suspensions during an impact event, since this would disrupt particle contact networks. **The earlier strain estimates for the impact conditions of the experiments suggest significant particle deformation for the cornstarch and silica particles.** It should be noted that the discrete elements in the computational model were considered to be purely elastic in their response, which influenced the computational result. Had the particles been able to deform or fracture, allowing them to slip past one another, then the conditions of the intergranular contacts would no longer be maintained due to these deformations, decreasing the effective force transfer within the particle bed. The computational model did demonstrate that intergranular friction was a primary factor in the kinetic energy ratio of the ejecta. A considerable drop in the α parameter would be correlated to a loss of frictional contact between particles. It would follow that a loss of interparticle friction increases with increasing impactor speeds is seen if particle deformations are considered. **This concept is shown graphically in Figure 11.**

The results from the impact face of the suspensions show a definite dependence of lateral stress transfer on the material properties of the suspended particles. The relative lateral kinetic energy of the ejecta decays faster with increasing projectile velocity in the purely silica-based suspension as opposed to the suspension with a significant proportion of silicon carbide mixed with the silica particles, **although both show similar trends.** At increasing impact velocities, the lateral stress transfer within the suspension reduces with increasing particle deformation. If we consider the added mass models explored in previous suspension impact work [18, 19], the present results provide some

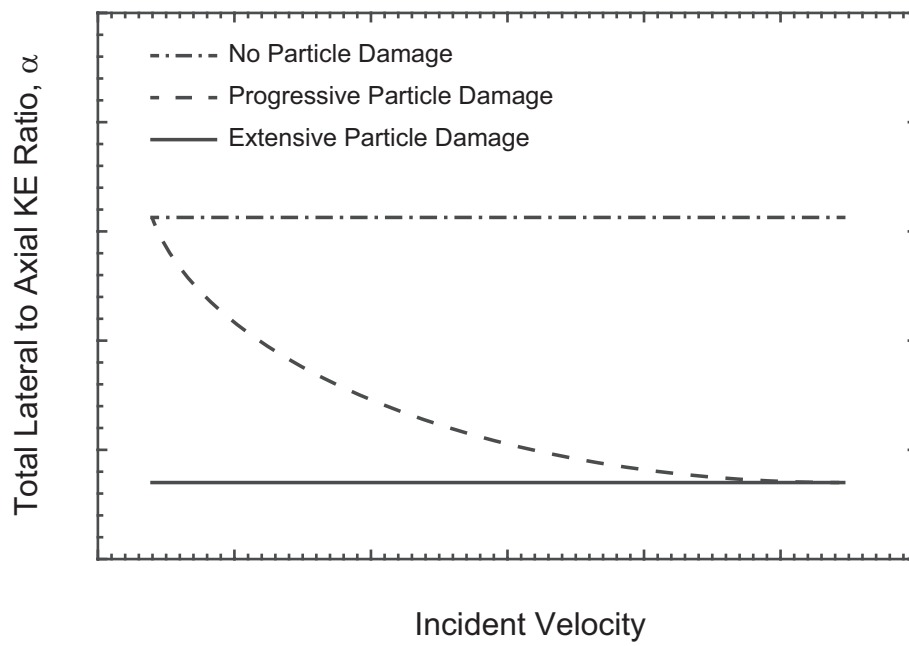


Figure 11: A conceptual interpretation of the results based on progressive particle damage.

evidence that the effects of this added mass response are progressively reduced with impact velocity, as may have been anticipated. At higher impact velocities, the deformation of particles at the periphery of the impact make the penetration mechanics resemble more closely to penetration driving a solid plug. This is consistent with analytical models that have been presented in previous ballistics work involving shear thickening fluids [29, 30]. This trend of reduced lateral stress transfer with increasing impact velocity is not visible in the cornstarch STF. However, when we consider that cornstarch is extremely malleable, having a Young's modulus that is an order of magnitude lower in comparison to either silica or silicon carbide [35], then we can be confident that any sustained contact between cornstarch particles will result in deformation at any of the impact velocities investigated (see strain estimates in Tables 2 and 3). Based on this hypothesis, the low material strength of the cornstarch explains the seemingly limited influence of friction and particle stiffness on its ejecta field, while the suspensions with high strength ceramics show a reducing influence of friction. At the highest impact velocities, the α parameter for the various STFs appear to converge, which may indicate that the role of friction within the suspensions at these stresses and strain rates is negligible or at least of an equivalent magnitude for all of three suspensions. While increasing the impact velocity will reduce the lateral stress transfer progressively within suspensions with hard particles as a larger proportion deform under dynamic loading, in materials where the strength of the particles are exceeded under all test conditions, the deformation of particles is not as strongly linked to the impact speed and the damage to lateral stress transfer capacity is not progressive.

6. Conclusions

A combined particle image velocimetry and image enhancement technique was developed to non-intrusively measure the velocity and mass of ejecta from ballistic impacts on fluid targets. The targets consisted of particle suspensions with several volume fractions and particles with different material properties.

A computational model was evaluated to investigate the role of particle surface roughness and stiffness on the ejecta field, with a particular focus on the lateral kinetic energy of the ejecta. The results of the ejecta measurements, 575 interpreted through the computational model **and particle strain estimates**, illustrate **the competing role of friction and particle strength** in the dynamic response of these suspensions **under ballistic loading**. The relationship between lateral stress transfer and projectile impact velocity was also used to show the role of particle stiffness on the response of these mixtures, **particu-** 580 **larly focusing on the effect of progressive damage among particles**. A drastic difference in ejecta behaviour was witnessed from a suspension with extremely soft cornstarch particles as opposed to the ejecta response of suspensions containing extremely hard ceramic particles, **which was interpreted as a result of the competition between intergranular friction, particle** 585 **stiffness, and particle deformation and fracture**. These experimental results provide evidence of the importance of considering interparticle frictional contacts **combined with particle damage models** in the dynamic response of shear thickening fluids, particularly in the ballistic regime of behaviour. **Future efforts will focus on introducing damage modelling into these** 590 **computational efforts to properly model the response of these fluids in extreme dynamic ranges**.

7. Acknowledgment

The authors would like to acknowledge the assistance of Jacques Blais of DRDC Valcartier in conducting the experimental investigations that were anal- 595 ysed in this paper. The authors would like to thank Charles Dubois and Behnam Ashrafi for their assistance in obtaining the rheological data. OE Petel would like to acknowledge funding support from the Natural Science and Engineering Research Council of Canada Discovery Grant program. JD Hogan would like to thank the financial support of US Army under grant ITOL TIP 2015-2443.

600 **8. References**

References

- [1] R. L. Hoffman, Discontinuous and dilatant viscosity behavior in concentrated suspensions. I. observations of a flow instability, *Transactions of the Society of Rheology* 16 (1972) 155–173.
- 605 [2] J. F. Brady, G. Bossis, The rheology of concentrated suspensions of spheres in simple shear flow by numerical simulation, *Journal of Fluid Mechanics* 155 (1985) 105–129.
- [3] H. A. Barnes, Shear-thickening (“dilatancy”) in suspensions of nonaggregating solid particles dispersed in newtonian liquids, *Journal of Rheology* 33 (2) (1989) 329–366.
- 610 [4] M. E. Cates, J. P. Wittmer, B. J.-P., P. Claudin, Jamming, force chains, and fragile matter, *Physical Review Letters* 81 (1998) 1841–1844.
- [5] A. J. Liu, S. R. Nagel, The jamming transition and the marginally jammed solid, *Annual Review of Condensed Matter Physics* 1 (2010) 347.
- 615 [6] E. Brown, H. M. Jaeger, The role of dilation and confining stresses in shear thickening of dense suspensions, *Journal of Rheology* 56 (2012) 875–923.
- [7] E. Brown, H. M. Jaeger, Shear thickening in concentrated suspensions: phenomenology, mechanisms and relations to jamming, *Reports on Progress in Physics* 77 (2014) 046602.
- 620 [8] S. P. Meeker, R. T. Bonnecaze, M. Cloitre, Slip and flow in soft particle pastes, *Physical Review Letters* 92 (2004) 198302.
- [9] D. Kalman, B. A. Rosen, N. J. Wagner, Effects of particle hardness on shear thickening colloidal suspension rheology, *The XVth international congress on rheology* (2008) 14081410.

- 625 [10] J. Mewis, N. J. Wagner, Colloidal suspension rheology, Cambridge University Press, 2012.
- [11] S. Jamali, A. Boromand, N. J. Wagner, J. Maia, Microstructure and rheology of soft to rigid shear-thickening colloidal suspensions, *Journal of Rheology* 59 (2015) 1377–1395.
- 630 [12] N. Fernandez, R. Mani, D. Rinaldi, D. Kadau, M. Mosquet, H. Lombois-Burger, J. Cayer-Barrioz, H. J. Herrmann, N. D. Spencer, Microscopic mechanism for the shear-thickening of non-Brownian suspensions, *Physical Review Letters* 111 (2013) 108301.
- [13] R. Seto, R. Mari, J. F. Morris, M. M. Denn, Discontinuous shear thickening
635 of frictional hard-sphere suspensions, *Physical Review Letters* 111 (2013) 218301.
- [14] J. E. Richardson, H. J. Melosh, C. M. Lisse, B. Carcich, A ballistics analysis of the Deep Impact ejecta plume: Determining Comet Tempel 1s gravity, mass, and density, *Icarus* 190 (2007) 357–390.
- 640 [15] N. J. Wagner, J. F. Brady, Shear thickening in colloidal dispersions, *Physics Today* 62 (10) (2009) 27–32.
- [16] B. J. Marazano, N. J. Wagner, The effects of particle size on reversible shear thickening of concentrated colloidal dispersions, *Journal of Chemical Physics* 114 (23) (2001) 10514–10527.
- 645 [17] D. Lootens, H. Van Damme, P. Hébraud, Giant stress fluctuations at the jamming transition, *Physical Review Letters* 90 (17) (2003) 178301.
- [18] S. R. Waitukaitis, H. M. Jaeger, Impact-activated solidification of dense suspensions via dynamic jamming fronts, *Nature* 487 (2012) 205–209.
- [19] S. R. Waitukaitis, L. K. Roth, V. Vitelli, H. M. Jaeger, Dynamic jamming
650 fronts, *Europhysics Letter* 102 (2013) 44001.

- [20] M. Roché, E. Myftiu, M. C. Johnston, P. Kim, H. A. Stone, Dynamic fracture of nonglassy suspensions, *Physical Review Letters* 110 (2013) 148304.
- [21] S. Mukhopadhyay, B. Allen, E. Brown, A shear thickening transition in concentrated suspensions under impact, arXiv:1407.0719.
- 655 [22] A. S. Lim, S. L. Lopatnikov, N. J. Wagner, J. W. Gillespie Jr., Investigating the transient response of a shear thickening fluid using the split hopkinson pressure bar technique, *Rheologica Acta* 49 (2010) 879–890.
- [23] O. E. Petel, A. J. Higgins, Shock wave propagation in dense particle suspensions, *Journal of Applied Physics* 108 (2010) 114918.
- 660 [24] O. E. Petel, D. L. Frost, A. J. Higgins, S. Ouellet, Lateral stress measurements in dense suspensions, *AIP Conference Proceedings* 1426 (1) (2012) 1495–1498.
- [25] O. E. Petel, D. L. Frost, A. J. Higgins, S. Ouellet, Formation of a disordered solid via a shock-induced transition in a dense particle suspension, *Physical Review E* 85 (2012) 021401.
- 665 [26] L. E. Gates Jr., Evaluation and development of fluid armor systems, Air Force Materials Laboratory, AFML-TR-68-362.
- [27] Y. S. Lee, E. D. Wetzel, N. J. Wagner, The ballistic impact characteristics of Kevlar woven fabrics impregnated with a colloidal shear thickening fluid, *Journal of Materials Science* 38 (13) (2003) 2825.
- 670 [28] D. P. Kalman, R. L. Merrill, N. J. Wagner, E. D. Wetzel, Effect of particle hardness on the penetration behavior of fabrics intercalated with dry particles and concentrated particle–fluid suspensions, *Applied Materials & Interfaces* 1 (11) (2009) 2602–2612.
- 675 [29] O. E. Petel, S. Ouellet, J. Loiseau, B. J. Marr, D. L. Frost, A. J. Higgins, The effect of particle strength on the ballistic resistance of shear thickening fluids, *Applied Physics Letters* 102 (2013) 064103.

- [30] O. E. Petel, S. Ouellet, J. Loiseau, D. L. Frost, A. J. Higgins, A comparison of the ballistic performance of shear thickening fluids based on particle strength and volume fraction, *International Journal of Impact Engineering* 85 (2015) 83–96.
- [31] J. Hogan, J. Spray, R. Rogers, G. Vincent, M. Schneider, Impact failure of planetary materials, *Experimental Mechanics* 54 (4) (2014) 665–675.
- [32] J. D. Hogan, J. G. Spray, R. J. Rogers, G. Vincent, M. Schneider, Dynamic fragmentation of planetary materials: Sub-hypervelocity ejecta measurements and velocity scaling, *Planetary and Space Science* 87 (2013) 66–77.
- [33] J. D. Hogan, J. G. Spray, R. J. Rogers, G. Vincent, M. Schneider, Dynamic fragmentation of natural ceramic tiles: Ejecta measurements and kinetic consequences, *International Journal of Impact Engineering* 58 (2013) 1–16.
- [34] J. D. Hogan, J. G. Spray, R. J. Rogers, G. Vincent, M. Schneider, Dynamic fragmentation of planetary materials: Ejecta length quantification and semi-analytical modelling, *International Journal of Impact Engineering* 62 (2013) 219–228.
- [35] S. R. Waitukaitis, Impact-activated solidification of cornstarch and water suspensions, Ph.D. Thesis - The University of Chicago, 2013.
- [36] G. M. Pharr, Measurement of mechanical properties by ultra-low load indentation, *Materials Science and Engineering A* 253 (1998) 151–159.
- [37] R. J. Adrian, Particle-imaging techniques for experimental fluid mechanics, *Annual Review of Fluid Mechanics* 23 (1991) 261–304.
- [38] R. J. Adrian, J. Westerweel, Particle image velocimetry, Vol. 30, Cambridge University Press, 2011.
- [39] R. C. Gonzalez, R. E. Woods, S. L. Eddins, Digital image processing using MATLAB, Pearson Education India, 2004.

- [40] G. S. Collins, K. Wunnemann, Numerical modeling of impact ejection processes in porous targets, *Lunar and Planetary Science* 38 (2007) 1789.
- 705
- [41] O. E. Petel, F. X. Jetté, Comparison of methods for calculating the shock Hugoniot of mixtures, *Shock Waves* 20 (2010) 73–83.
- [42] K. Wada, H. Senshu, T. Matsui, Numerical simulation of impact cratering on granular material, *Icarus* 180 (2006) 528–545.
- 710
- [43] LSTC, LS-DYNA Keyword User’s Manual R7.1, Livermore Software Technology Corporation (LSTC), 2014.